Geophysical and Astrophysical Fluid Dynamics
Vol. ??, No. ?, ???, 200?, pp. 1–17

Taylor & Francis
Taylor & Francis Group

MAGNETIC TOPOLOGIES IN THE SOLAR CORONA DUE TO FOUR DISCRETE PHOTOSPHERIC FLUX REGIONS

C. BEVERIDGE*, E.R. PRIEST and D.S. BROWN

Mathematical Institute, University of St Andrews, North Haugh, St Andrews KY16 9SS, UK

(Received 21 July 2003; In final form 29 March 2004)

Many dynamic phenomena in the solar corona are driven by the complex and ever-changing magnetic field. It is helpful, in trying to model these phenomena, to understand the structure of the magnetic field, i.e. the magnetic topology. We study here the topological structure of the coronal magnetic field arising from four discrete photospheric flux patches, for which we find that seven distinct, topologically stable states are possible; the changes between these are caused by six types of bifurcation. Two bifurcation diagrams are produced, showing how the changes occur as the relative positions and strengths of the flux patches are varied. A method for extending the analysis to higher numbers of sources is discussed.

Keywords: Solar corona; Magnetic field; Topology

1. INTRODUCTION

The magnetic energy in the solar corona is, generally, by far the strongest form of energy. It follows that many dynamic coronal phenomena – including, for instance, solar flares and eruptive prominences – are driven magnetically.

The magnetic field is believed to arise from a large number of intense, isolated flux sources in the photosphere. These are commonly interpreted as locations where flux tubes originating in the solar interior break through the surface and spread out into the atmosphere.

This field, even from a handful of stationary sources, is immensely complicated. In reality, there are many thousands of sources constantly moving around, emerging and disappearing, combining and fragmenting and growing or shrinking in strength and size (Berger *et al*., 1998; Parnell, 2001) all of which complicate the coronal field structure further. Topological methods are beginning to achieve a basic understanding of such complex fields.

Many of the dynamic phenomena in the corona occur only in complex configurations when topologically distinct parts of the magnetic field are interacting with each other

*Corresponding author. E-mail: colinb@mcs.st-and.ac.uk

ISSN 0309-1929 print: ISSN 1029-0419 online © 200? Taylor & Francis Ltd
DOI: 10.1080/0309192041000171557 5

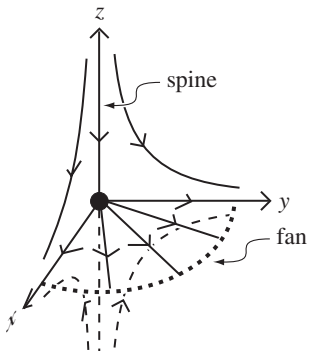

FIGURE 1 The local structure of a magnetic null. In one direction, the field lines cluster around an isolated field line known as the spine; perpendicular to this, the lines spread out in a fan plane. The field lines of this fan plane form a separatrix surface, which generally divides space into regions of different connectivity.

1

(e.g., in flares, Démoulin *et al*., 1992; Lau, 1993; Aulanier *et al*., 1998; Fletcher *et al*., 2001).

An important long-term project is to categorize and study the different types of topology of the coronal magnetic field as a prerequisite for a full understanding of the mechanisms, which control dynamic phenomena such as flares and loop structures.

In this article, our aim is to focus on a simple class of complex topologies that often occurs in a solar active region, namely the field due to four balanced flux sources. This scenario is of some importance, since it includes the two-bipole situation (Beveridge *et al*., 2002) that arises when a new bipole emerges into a preexisting bipolar region, and the more generic case (studied here) where flux cancellation has occured and the region can no longer be described by a pair of dipoles.

We describe the complexity of a configuration by calculating the *magnetic skeleton* of the field (Priest *et al*., 1997). This consists of the positions of the sources and any null points, along with their spine field lines and fan separatrix surfaces, as well as any separators (all of which are defined in Section 2).

The arrangement of these features determines their topology. We examine here the topologies due to four discrete point sources, following for instance Gorbachev *et al*. (1988). They gave a preliminary treatment of four sources and found that a coronal null can exist in such a configuration and that a separator does not occur in every case.

This study complements the work undertaken by Priest *et al*. (1997), on two-source and simple three-source cases, by Brown and Priest (1999), who completely classified the three-source scenario, and by Beveridge *et al*. (2002), who examined the two-bipole case.

Brown and Priest (1999) detailed eight possible topologies in the unbalanced three-source case, and analyzed the bifurcations among them. We will return to their analysis later.

In Section 2, we outline our assumptions and the model adopted. We begin by discussing the topologies found in Section 3; the (four source) intersecting, detached, nested and coronal null states have been explored in earlier papers, but the upright null, enclosed and separate states are new.

+ [NT: 248×174mm] Ver: 7.51g/w [13.5.2004–3:48pm] FIRST PROOFS {GandB}Ggaf/GGAF-41015.3d Geophys. Astrophys. Fluid Dynamics (GGAF) Paper: GGAF-41015 Keyword

We show how the configuration can change between these states in Section 4 by reviewing the bifurcations that take place. We then detail bifurcation diagrams showing the parameter values at which the bifurcations occur.

We conclude the article with a discussion of our results, and a comparison with previous findings, in particular those of Brown and Priest (1999).

2. THE MAGNETIC CHARGE TOPOLOGY MODEL AND SKELETONS

2.1. Magnetic Charge Topology

We use the assumptions of *Magnetic Charge Topology* (MCT) (see, for instance, Longcope, 1996), where photospheric flux patches are modeled as point sources, since the field at a distance r from a flux patch of nonzero radius R does not differ significantly from that of a point source when $r \gg R$. The coronal magnetic field is often considered to be force-free, and since we are studying the topology of the field, we will, for simplicity, make the further assumption that the field is potential – that is, that the magnetic field $\mathbf{B}$ can be written as $-\nabla\Phi$, where Φ is a scalar potential. Force-free fields, at least at low shear, are unlikely to have any different topological states, although the parameter values at which changes between states occur will generally depend on how far is the field from the potential (Brown and Priest, 2000). In general, coronal fields can display behavior far more complex than that shown here; a potential field is a first step towards understanding such behavior.

For a set of n discrete sources located at $\mathbf{r}_i$ with strengths ϵ_i $(i = 1, \ldots, n)$, the potential magnetic field is given by

$$\mathbf{B}(\mathbf{r}) = \sum_{i=1}^{n} \epsilon_i \frac{\mathbf{r} - \mathbf{r}_i}{|\mathbf{r} - \mathbf{r}_i|^3}. \tag{1}$$

The sources lie in the photosphere, which we model locally as a plane, taking the corona to be the half-space above it; in this article, we focus on the case where $n = 4$ and $\epsilon_4 = -(\epsilon_1 + \epsilon_2 + \epsilon_3)$ to ensure flux balance. Without loss of generality, we can rescale the geometry by choosing two of the source locations as $\mathbf{r}_1 = (0, 0, 0)$ and $\mathbf{r}_2 = (1, 0, 0)$. We can also rescale the source strengths so that $\epsilon_1 = 1$. This scaling reduces the twelve-dimensional parameters in the original problem to just six independent (dimensionless) parameters.

Our new expression for $\mathbf{B}(\mathbf{r})$ is then

$$\mathbf{B}(\mathbf{r}) = \frac{\mathbf{r}}{|\mathbf{r}|^3} + \epsilon_2 \frac{\mathbf{r} - \hat{\mathbf{x}}}{|\mathbf{r} - \hat{\mathbf{x}}|^3} + \epsilon_3 \frac{\mathbf{r} - \mathbf{r}_3}{|\mathbf{r} - \mathbf{r}_3|^3} - (1 + \epsilon_2 + \epsilon_3) \frac{\mathbf{r} - \mathbf{r}_4}{|\mathbf{r} - \mathbf{r}_4|^3}. \tag{2}$$

The six parameters are the values of ϵ_2 and ϵ_3 and the coordinates of $\mathbf{r}_3$ and $\mathbf{r}_4$ in the $z = 0$ plane. This is still too many parameters to allow for a comprehensive study, so we consider here the effects of fixing $\mathbf{r}_3$, ϵ_2 and ϵ_3 while allowing the fourth source to move freely.

Null points are locations at which the magnetic field vanishes. Their local structure has been examined in detail, for instance by Parnell *et al.* (1996), and is depicted in

Fig. 1. A coordinate system can be chosen such that the first-order linear field near a magnetic null can be written as $\mathbf{B} = \mathbf{M} \cdot \mathbf{r}$, where $\mathbf{r} = (x, y, z)^T$ and

$$\mathbf{M} = \begin{pmatrix} \partial B_x/\partial x & \partial B_x/\partial y & \partial B_x/\partial z \\ \partial B_y/\partial x & \partial B_y/\partial y & \partial B_y/\partial z \\ \partial B_z/\partial x & \partial B_z/\partial y & \partial B_z/\partial z \end{pmatrix} = \begin{pmatrix} 1 & \frac{1}{2}(q - j_\parallel) & 0 \\ \frac{1}{2}(q + j_\parallel) & p & 0 \\ 0 & j_\perp & -(p+1) \end{pmatrix}, \quad (3)$$

where $j_\parallel$ and $j_\perp$ represent components of the current parallel and perpendicular to the spine, respectively, while p and q are parameters of the potential field. In this article, will be considering the potential situation, where $j_\parallel$ and $j_\perp$ are equal to zero. The solenoidal condition $\nabla \cdot \mathbf{B} = 0$ implies that the trace of the matrix $\mathbf{M}$ in (3) vanishes, and hence so does the sum of its eigenvalues. Ignoring the degenerate cases, when one or more of the eigenvalues is equal to zero, it is clear that one of the eigenvalues (λ_1) is of the opposite sign to the other two (λ_2 and λ_3). We label their corresponding eigenvectors as $\mathbf{e}_1$, $\mathbf{e}_2$ and $\mathbf{e}_3$, respectively. These eigenvectors are crucial to the skeleton.

The eigenvector associated with the odd-signed eigenvalue, $\mathbf{e}_1$, defines two isolated field lines known as *spines* (Priest and Titov, 1996). If $\lambda_1 > 0$, these are directed away from the null point, and if $\lambda_1 < 0$, they are directed towards it. These field lines end (or begin) in sources called *spine sources*

Together, $\mathbf{e}_2$ and $\mathbf{e}_3$ define a *fan plane*. Points lying in this plane near to the null define field lines which form a *separatrix surface* (also called the *fan*), which usually divides space into regions of different *connectivity*. The only exception to this is when both spines of a null point connect to the same source; otherwise field lines on different sides of the surface either start from or end at the two spine sources. Separatrix surfaces are categorized into *domes*, *walls* and *part-walls*. Separatrix domes are surfaces bounded by a closed curve in the photosphere; walls are bounded by at least one curve stretching to infinity. Part-walls are separatrices bounded by a finite curve which does not lie entirely in the photosphere.

Quasi-separatrix layers (QSLs) (see, for instance, Démoulin *et al.*, 1999; Titov and Horing, 2002), are layers across which the connectivity changes sharply but continuously. Separatrices are limiting cases of this in which the connectivity is discontinuous.

If λ_2 and λ_3 are positive, the fan field lines diverge from the null point; if the eigenvalues are negative, these field lines converge on the null. The null is called *positive* if λ_2 and λ_3 are both positive, or *negative* if both are negative. For coplanar photospheric sources, there is necessarily a population of nulls which lie in this plane, called *photospheric nulls*. A photospheric null point whose spine lies in the plane of the sources is described as *prone*, whereas a photospheric null with a spine directed vertically is called *upright*.

In a situation with flux balance, the field at a great distance from the sources is approximately dipolar. On a contour of sufficiently large diameter, the Kronecker–Poincaré index of the field χ will be two (Molodenskii and Syrovatskii, 1977). The Euler characteristic equation $M - c + m = \chi$ then holds in the photospheric plane, where M is the number of potential maxima (see, for instance, Inverarity and Priest, 1999); m is the number of minima and c is the number of saddle points. Saddle points of the potential correspond to prone nulls; maxima (respectively, minima) correspond either to positive (respectively, negative) sources or to positive (respectively, negative) upright nulls.

This allows us to relate the numbers of sources (S), prone nulls (n_p) and upright nulls (n_u) by the two-dimensional Euler characteristic equation,

$$S + n_u = n_p + 2, \tag{4}$$

when the net flux in the source plane is zero. The properties of nulls in the three-dimensional space are governed by the three-dimensional Euler characteristic equation,

$$S_+ - n_+ = S_- - n_-, \tag{5}$$

where $S_\pm$ represents the number of positive or negative sources and $n_\pm$ the number of positive or negative nulls. In both of these equations, flux balance is assumed.

Separators are field lines which begin at one null point and end at another. They are the three-dimensional analog of a two-dimensional X-point but with a component in the third dimension, and are prime locations for reconnection (Lau and Finn, 1990; Priest and Titov, 1996; Galsgaard and Nordlund, 1997; Gorbachev *et al.*, 1998). Separators usually represent the boundary of four different regions of connectivity, and are a limiting case of the hyperbolic flux tube (Titov *et al.*, 2002) the intersection of two quasi-separatrix layers.

2

A three-source case displaying sources, null points, fans, spines and a separator is shown in Fig. 2.

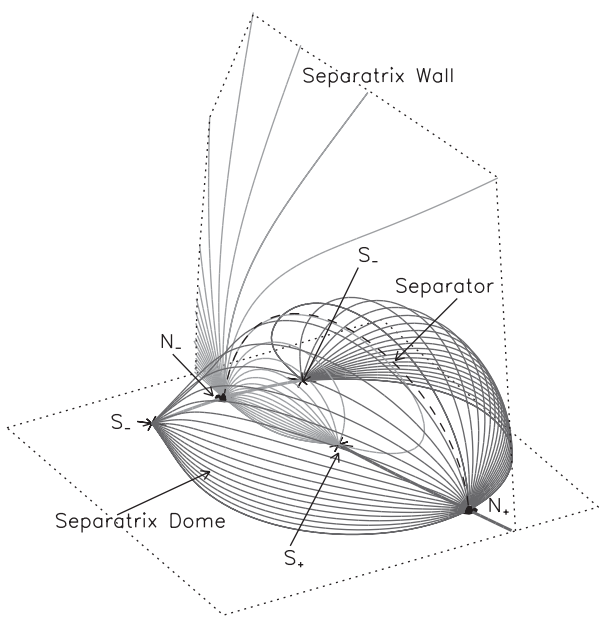

FIGURE 2 A typical three-source topology – the intersecting case. The stars represent positive and negative sources, labeled as S+ and S−, respectively. The large dots labeled as N+ and N− are positive and negative null points, respectively. The dashed line is a separator, which is the line of intersection between two separatrix surfaces (containing the lighter solid field lines) which here form a dome and a wall. The thick solid lines are spine field lines.

3. TOPOLOGIES

The different possible connectivities of the fan and spine field lines define the different topologies of the overlying coronal magnetic configuration.

By using the Euler characteristic equations (4) and (5), we see that there must be two more prone nulls than upright nulls. This implies that the number of photospheric nulls is even in a four-source setup. In most cases, there are two photospheric nulls, although the upright null state (Section 3.2) has four.

In a situation with three sources of one polarity (say, positive) and one of the other parity, (5) dictates that there be two more positive nulls than negative; if there are two sources of each polarity, there must be as many positive as negative nulls.

Information on possible topologies can be obtained by the use of domain graph method introduced by Longcope (1996). In this, each flux source is represented as a vertex of a graph, and an edge connects two vertices if and only if field lines connect the two corresponding sources. It is evident that a pair of vertices cannot be joined unless the sources they represent are of opposite sign. It can be shown that this graph (except in highly-symmetric cases) is connected.

Given these conditions, there are only three possible graphs to represent the three-source case, as shown in Fig. 3. If three sources are of the same sign (say, positive), only one graph is possible: every positive source connects to the negative source. Two graphs are admissible when the source polarities are evenly split: one in which each positive source connects to each negative source, and one in which an edge is missing.

These graphs correspond to three classes of topology, each with its own connectivity pattern. Within each class, the topology can only change by means of a bifurcation with no effect on connectivity: all of the bifurcations described in the following section are possible, with the exception of the global separator bifurcation (in which a flux domain is created or destroyed). For each class, it suffices to find a sample topology and consider how it can bifurcate.

For instance, the third scenario, where three flux domains exist, is satisfied by the detached state. We consider the possible bifurcations, and find that neither local bifurcation is possible, since no separator exists and only two sources of either polarity exist. The global spine–fan bifurcation cannot occur because it requires two nulls of the same sign. This leaves the two global quasi-bifurcations, both of which can occur. The global separatrix quasi-bifurcation changes the configuration into the nested state, but the global spine quasi-bifurcation has no effect on the topology.

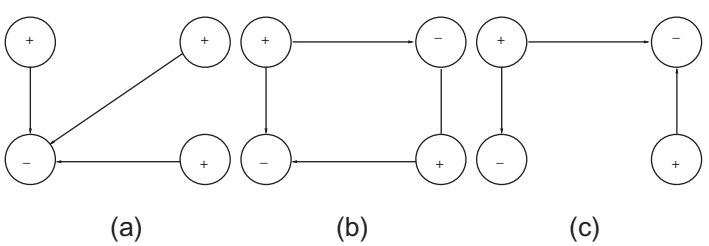

FIGURE 3 Possible domain graphs for four sources. (a) If three sources are of the same polarity, all must connect to the opposite source. If there are two sources of either polarity, either (b) each positive source connects to each negative source or (c) one positive–negative pair remains unconnected.

Repeating the analysis for the nested state, we find that these are the only possible topologies for the third class. We apply the same method to the remaining two classes and find that only the following topologies are possible.

3.1. Separate and Enclosed States

The separate and enclosed states occur only when three of the sources are of one sign and the remaining source is of the other. In both cases (Figs. 4 and 5), two separatrix domes exist, each surrounding one of the positive sources and connecting to the negative source. In the separate state, the two domes are independent; in the enclosed state, one of the domes surrounds the other.

These are very similar to the three-source separate and enclosed states; the only difference is that, where a spine in the three-source scenario is connected to infinity, here it connects to a third positive source. These two cases also subsume the divided state; whereas both separatrices in that state connect to infinity, here, both connect to a source.

3.2. Upright Null State

The upright null state (Fig. 6) occurs only when three of the sources are of the same sign. In it, three prone nulls and an upright null exist. The fan of the upright null lies in the plane and is bounded by the spines of the prone nulls; its spine connects to the negative source above and below the plane. The spine bounds all of the separatrix surfaces from the prone nulls, two of which form part-domes, and the other a bounded wall. Three photospheric separators connect the upright null to the surrounding prone nulls.

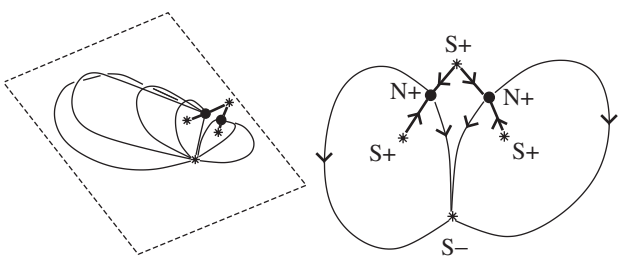

FIGURE 4 Separate state. Two independent separatrix domes meet only at the negative source.

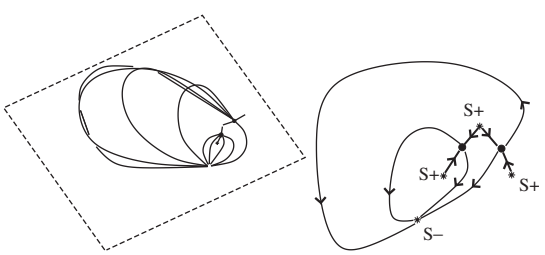

FIGURE 5 Enclosed state. Two separatrix domes meet only at the negative source; one is entirely enclosed by the other.

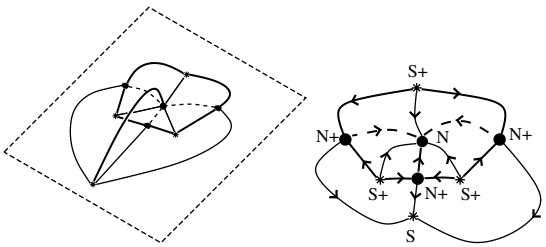

FIGURE 6 Upright null state. There are three separatrix surfaces from positive nulls (N+): two form part-domes bounded by the spine of the upright null (N−), while the other is a wall, also bounded by the spine. The separatrix of the negative null lies entirely in the plane and is bounded by the spine field lines of the positive nulls.

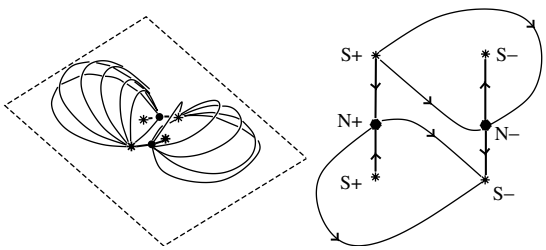

FIGURE 7 Detached state. The two separatrix domes do not intersect. There is no separator and only three regions of connectivity.

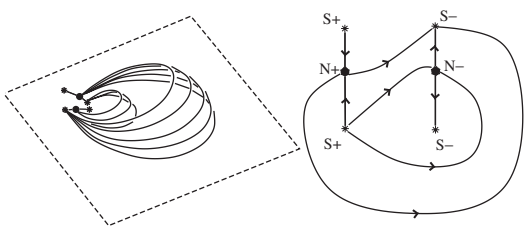

FIGURE 8 Nested state. One separatrix dome surrounds the other. There are three regions of connectivity and no separator exists. These are schematic plots; in practice, both separatrix domes are often much larger than they appear here.

This is similar to both the touching and triangular states in the three-source scenario; in both of those cases, either separatrices or spines connect to infinity. Here, they connect to a source.

3.3. Detached and Nested States

The detached (Fig. 7) and nested (Fig. 8) states occur when two of the sources are positive and two negative. If all of the fan field lines from one null connect to one source and all those in the other fan connect to the other, the state is one of these two. The only difference between them is that in the nested state, one of the separatrix domes envelops the other, while the detached state is topologically identical to two independent and unbalanced pairs of sources.

These two states are very similar to the three-source detached and nested states; in those situations, one of the separatrix surfaces is connected to infinity; here, the surfaces connect to a source.

3.4. Intersecting State

The intersecting state occurs if the fan field lines for a null in the plane connect to different sources, and the nulls are of different signs (Fig. 9). The fans of the two nulls here form two separatrix domes, which intersect in a separator field line.

This is quite similar to the three-source intersecting state; there, the separatrix wall connected to infinity; here, it connects to a fourth source.

3.5. Coronal Null State

Finally, if both nulls are of the same sign, a further two nulls of the opposite sign are required to satisfy the three-dimensional Euler characteristic equation. Because of the symmetry in the plane, one must be above the photosphere (i.e. a coronal null) and the other in the unphysical region $z < 0$, below the photosphere. This is the coronal null state (Fig. 10.)

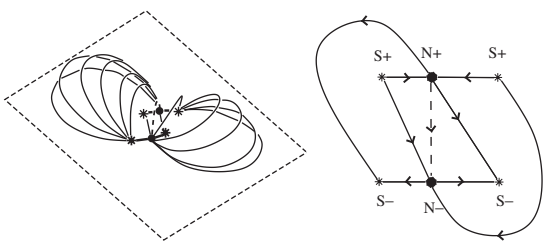

FIGURE 9 Intersecting state. The separatrices form domes which intersect in a separator. There are four distinct regions of connectivity.

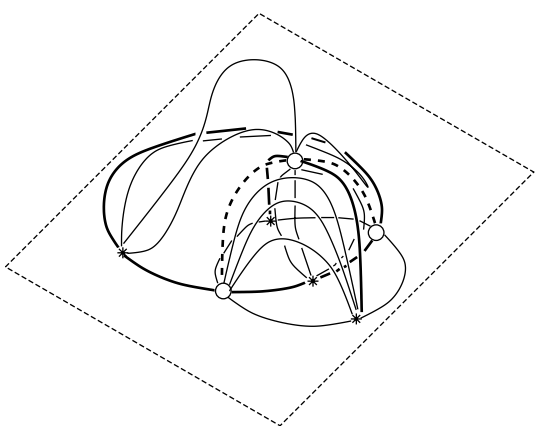

FIGURE 10 Coronal null state. There are four regions of different connectivity and two separators, each of which is a field line joining the coronal null to a null in the photospheric plane.

This state has no three-source analog; in fact, it can be shown that coronal nulls exist only in structurally unstable null rings in the unbalanced three-source case.

4. BIFURCATIONS

The bifurcations considered in this section belong to one of the two types: *global* bifurcations, in which the overall structure of the field changes without changing the number of nulls; and *local* bifurcations, in which the null points are created or destroyed. Local bifurcations may, and almost always do, have global properties.

There are six types of bifurcation, of which two are local: the local separator bifurcation which is a generalization into three dimensions of a classical saddle-node bifurcation; and the local double-separator bifurcation, which is an extension of the pitchfork bifurcation. The remaining four are global: the global spine–fan and global separator bifurcations are variants on the heteroclinic bifurcation while the global separatrix and global spine quasi-bifurcations display no finite bifurcation behavior. We rename these classical bifurcations for the better representation of the changes they cause to the magnetic field, as well as to reflect the fact that they display slightly different behavior in three dimensions, and different variations of an individual classical bifurcation can occur.

4.1. Local Separator Bifurcation

The local separator bifurcation was studied in detail, and modeled analytically, by Brown and Priest (1999). During such a bifurcation, two null points either spontaneously appear or collide and annihilate each other. Equation (5) insists that the two nulls be of opposite sign. If the bifurcation takes place in the plane – which is more usual – then (4) forces one of the nulls to be prone and the other upright.

The process is illustrated in Fig. 11. A second-order null (D) appears out of nothing in the second frame; it then splits into two nulls (N2 and N3). Eventually, N2 will annihilate N1 in the reverse process, leaving only the N3. It is believed, although no proof is known, that the local separator bifurcation requires at least three sources of the same polarity to take place.

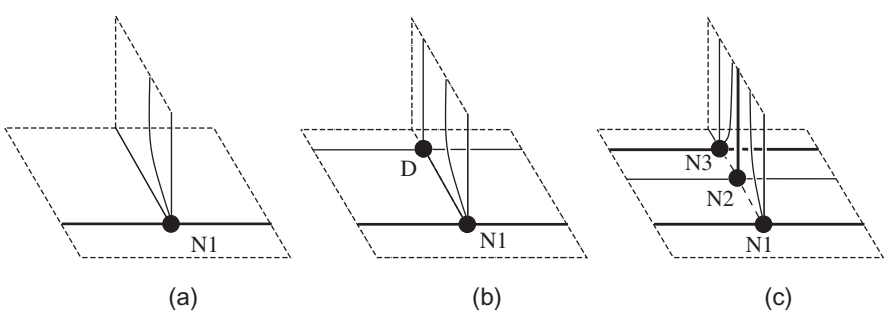

FIGURE 11 Local separator bifurcation. In (a) a single null point (dot N1) exists. In (b) a second-order null (dot D) comes into existence. This splits into two nulls (N2 and N3) (c). These two nulls are linked by a separator (dashed line). Thick and thin solid curves represent spine and fan field lines, respectively; the dashed line between N1 and N2 is also a separator created by the bifurcation, but is not strictly part of the bifurcation.

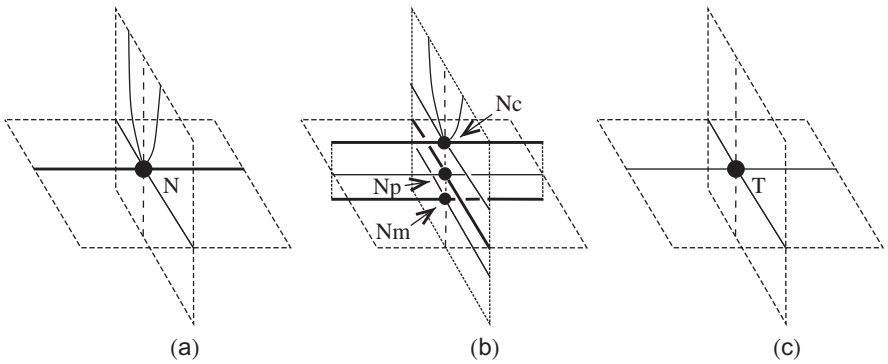

FIGURE 12 Local double-separator bifurcation. In (a) a single first-order null (N) exists; in (b) it becomes a third-order null (T). In (c) the null has split into three first-order nulls: one (Nc) above the photosphere; one (Np) on the photosphere; and one (Nm) below the photosphere. The three new nulls are linked by separators (dashed lines).

4.2. Local Double-separator Bifurcation

The local double-separator bifurcation was analyzed by Brown and Priest (2001), who provided an analytical model for it. In it, a null point becomes a third-order null before splitting into three first-order nulls. This type of bifurcation requires a high degree of symmetry, such as that provided by the photosphere, which provides a mirror corona for $z < 0$. It seems unlikely that such a bifurcation would take place anywhere other than on the photosphere, creating one *coronal null* (one lying above the photosphere) and a mirror image null below the photosphere. By symmetry, the coronal null and its mirror image must be of the same sign; the three-dimensional Euler characteristic equation (5) insists that both of these nulls be of the sign of the original photospheric null, and that the photospheric null change sign. It is believed, although no proof is known, that this bifurcation takes place only on an existing separator.

The process is illustrated in Fig. 12. A single null becomes three, creating two new separators.

4.3. Global Spine–Fan Bifurcation

The global spine–fan bifurcation is discussed in Brown and Priest (1999). It allows a spine field line connecting to one source and a separatrix connecting to another swap connectivities. This process is shown in Fig. 13. The spine and fan involved in the bifurcation originally connect to different sources (Fig. 13a); the two approach, until the spine lies in the fan surface. At the moment of bifurcation (Fig. 13b), the spine technically forms a separator because it connects the two null points; however, this configuration is structurally unstable. As the process continues, the spine passes through the fan to connect to a different source; likewise, the fan now connects to the source originally connected to the spine.

4.4. Global Separator Bifurcation

The global separator bifurcation, in which a separator is destroyed or created, is well understood (Brown and Priest, 1999). Figure 14 shows an example of this. In (Fig. 14a) there are two separatrix domes intersecting in a separator. As the two

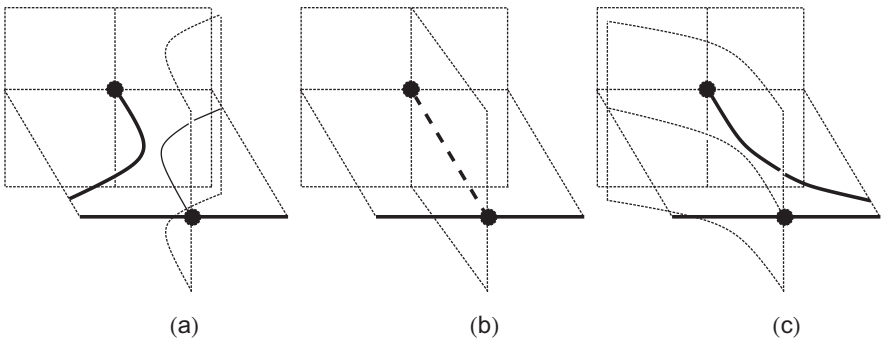

FIGURE 13 Global spine–fan bifurcation. (a) The spine of the more distant null initially connects to the left of the configuration, and the fan of the nearer null connects to the right. The two approach each other until (b) the spine lies in the fan plane. By this process, the fan and spine swap connectivities (c). This bifurcation requires two nulls of the same sign.

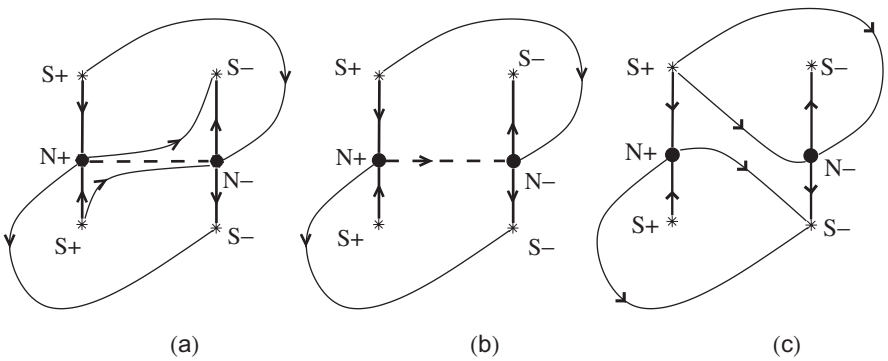

FIGURE 14 Global separator bifurcation. The intersecting separatrix surfaces approach each other (a), and the separator drops in height. At the point of bifurcation, the separator lies in the plane (b) before vanishing (c); there are now two detached separatrix surfaces.

domes move apart, the separator falls in height until, at the moment of bifurcation (Fig. 14b), it reaches the plane and vanishes, to leave the detached topology (Fig. 14c).

4.5. Global Separatrix Quasi-bifurcation

In the global separatrix quasi-bifurcation, discussed in Beveridge *et al*. (2002), a separatrix grows infinitely large and wraps around to the other side of the configuration. The process is shown in Fig. 15. One separatrix dome grows progressively larger until it extends to infinity and becomes a separatrix wall. The separatrix wall still divides the space into two distinct regions, but does not enclose either of them. After the bifurcation, the field lines connect again with the same source, but on the other side of the system, in such a way that the separatrix dome now encloses a different source.

We refer to this as a quasi-bifurcation because one of the features of the skeleton (in this case the separatrix surface) moves off to infinity, as opposed to regular bifurcations where the skeleton is altered within a bounded region. When this movement to infinity happens, there may be a change of topological state from one type to another (as in the

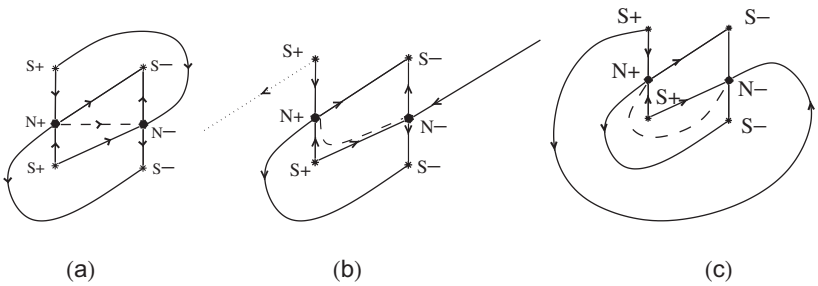

FIGURE 15 Global separatrix quasi-bifurcation. One of the separatrix domes grows in size (a) until it becomes a separatrix wall (b) and eventually wraps around the other (c).

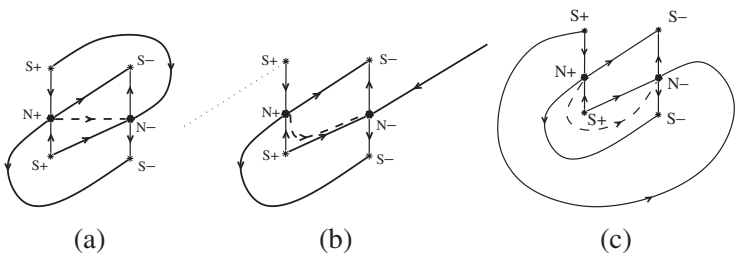

FIGURE 16 Global spine quasi-bifurcation. (a) One separatrix surface containing a spine, grows until it forms a separatrix wall (b) and eventually wraps around to the other side of the configuration (c).

change from an enclosed state to a nested state in the four-source case Beveridge *et al.*, 2002)); or, as in the present case, there may be a change of handedness from one state to another distinct state of the same type. Here the left and right states in Figs. 15(a,c) are indeed distinct because the separatrix domes enclose different sources. However, there is no regular bifurcation behavior in any bounded region.

4.6. Global Spine Quasi-bifurcation

The global spine quasi-bifurcation (Beveridge *et al.*, 2002) is depicted in Fig. 16. It is effectively identical to the global separatrix quasi-bifurcation except that the separatrix involved contains the spine field line of the other null.

5. BIFURCATION DIAGRAMS

Let us consider the arrangements of sources that produce the various topological states. We begin by fixing three sources and allowing a fourth, balancing source, to move freely around the source plane; its coordinates are $(x_4, y_4, 0)$.

From each such configuration, we find the null points, and follow fan field lines from each of the nulls numerically. By analyzing the connectivity of these field lines, it is possible to determine the topology for a given set of sources. In doing so, we find the values of parameters x_4 and y_4 where bifurcations occur and join them with smooth curves.

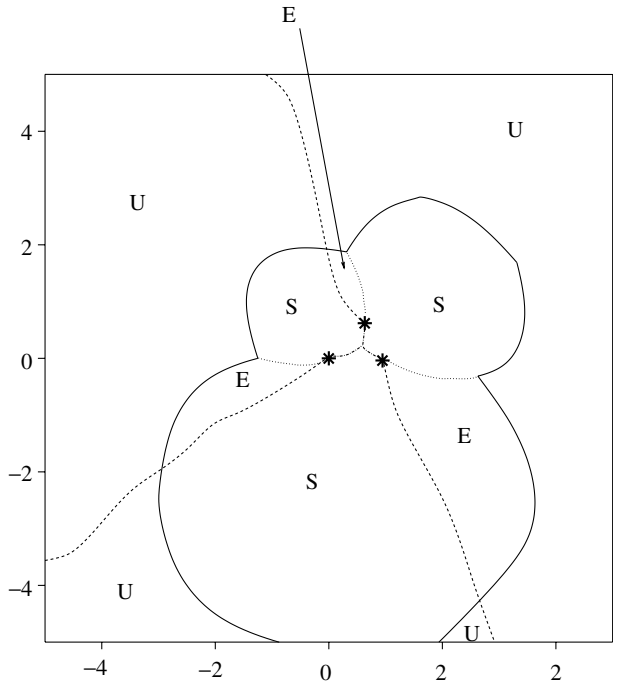

FIGURE 17 Bifurcation diagram for three positive sources. Three sources are fixed at $\mathbf{r}_1 = (0, 0, 0)$, $\mathbf{r}_2 = (1, 0, 0)$ and $\mathbf{r}_3 = (0.7, 0.6, 0)$, with strengths $\epsilon_1 = 1$, $\epsilon_2 = 0.6$ and $\epsilon_3 = 0.5$. A fourth balancing source with strength $\epsilon_4 = -2.1$ is allowed to move freely. The different regions on the plot indicate where the fourth source must be placed to give these topologies. The lines represent bifurcations: a solid line represents a local separator bifurcation, and a dotted line a global spine–fan bifurcation. Dashed lines are global separatrix quasi-bifurcations, while dot–dashed lines represent global spine quasi-bifurcations. The topological states are represented by letters: U (upright), E (enclosed) and S (separate).

In Fig. 17, we analyze a balanced case with one negative and three positive sources. We find that, when the moving source is far from the fixed sources, the topology is invariably in the three-source state associated with the other, central sources – in this case the *upright null* state (see Section 3.2); closer in, the field adopts a *separate* or an *enclosed* topology (Section 3.1). The *local separator bifurcation* (Section 4.1) forms the boundary between these two regions.

Each enclosed region touches a source, and is bounded on either side by a *global separatrix* and a *global spine quasi-bifurcation* (Sections 4.5 and 4.6)

Lastly, the boundaries between the three separate regions, which occur when the fourth source is (in some sense) between the three others, are formed by the *global spine–fan bifurcation* (Section 4.3).

In Fig. 18, we do the same thing for a balanced case with two positive and two negative sources. When the moving source is distant from the sources, or between them, the field is in the *intersecting* state (Section 3.4). A *global separator bifurcation* (Section 4.4) separates these regions from the *nested* and *detached* regions (Section 3.3), which in turn are separated by a global separatrix quasi-bifurcation.

There is also a region in which the topology has a *coronal null* (Section 3.5); this touches two of the sources and is divided from the intersecting region by a *local double-separator bifurcation* (Section 4.2), marked by a dashed line.

+ [NT: 248×174mm] Ver: 7.51g/w [13.5.2004–3:48pm] FIRST PROOFS {GandB}Ggaf/GGAF-41015.3d Geophys. Astrophys. Fluid Dynamics (GGAF) Paper: GGAF-41015 Keyword

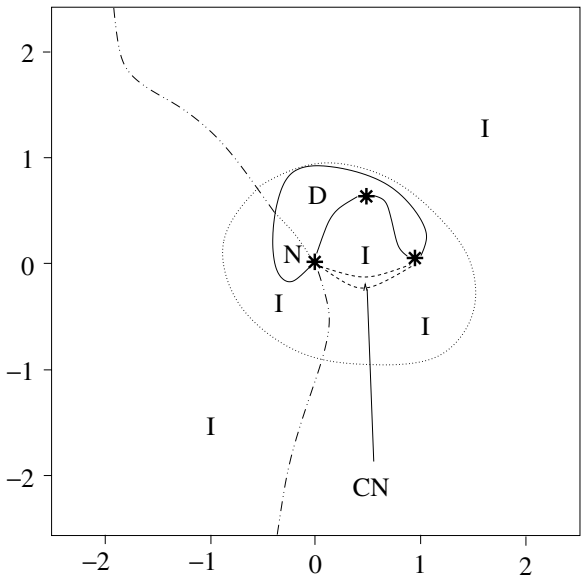

FIGURE 18 Bifurcation diagram for a bipolar case. Three sources are fixed at $\mathbf{r}_1 = (0, 0, 0)$, $\mathbf{r}_2 = (1, 0, 0)$ and $\mathbf{r}_3 = (0.7, 0.6, 0)$, with strengths $\epsilon_1 = 1$, $\epsilon_2 = 0.6$ and $\epsilon_3 = -0.6$. A fourth balancing source with strength $\epsilon_4 = -1.0$ is allowed to move freely. The different regions on the plot indicate where the fourth source must be placed to give these topologies. The lines represent bifurcations: a solid line represents a global separator bifurcation, and a dashed line a local double-separator bifurcation. A dotted line represents a global separatrix quasi-bifurcation, and a dash–double-dotted line a global spine quasi-bifurcation. The four possible topologies are denoted by letters I (intersecting), D (detached), N (nested) and CN (coronal null).

There is a further global separatrix quasi-bifurcation line which surrounds the sources and divides one intersecting state from another. Lastly, a global spine quasi-bifurcation line passes through the source at the origin; outwith the intersecting region, this becomes a global separatrix quasi-bifurcation.

The resulting bifurcation diagrams (Figs. 17 and 18) are rather complicated and include all six permissible types of bifurcation (namely, a global separator bifurcation, a global spine–fan bifurcation, a local separator bifurcation, a local double-separator bifurcation, a global separatrix quasi-bifurcation and a global spine quasi-bifurcation, described in Section 4). They allow changes among all seven possible topological states: in a situation with three sources of one sign and one of the other, three topologies (namely, the separate, enclosed and upright null states) are possible; if there are two sources of each polarity, then four states (the detached, nested, intersecting and coronal null states) are possible.

Calculating the bifurcation diagrams is made particularly difficult by the global separatrix and the global spine quasi-bifurcations, in which parts of the skeleton move off to infinity and are not easily found by automatic computational algorithms.

6. DISCUSSION

In reality, the solar surface contains many flux patches in the form of sunspots, ephemeral regions, network elements and intense flux tubes, which constantly

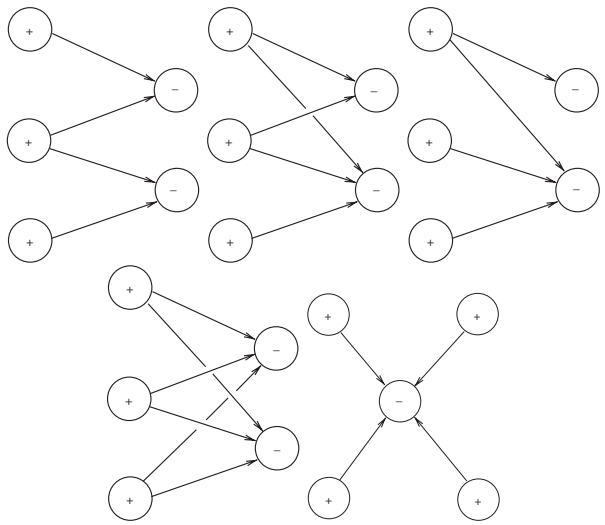

FIGURE 19 Five-source domain graphs. Five distinct graphs are permissible.

appear, fragment, merge, cancel and disappear. The resultant overlying coronal field is massively complex.

As a starting point for understanding its structure, finding the possible topologies due to smaller numbers of sources is important, since these act as building blocks for the full field. Before now, the unbalanced three-source case had been completely catalogued by Brown and Priest (1999), and an analysis of the two-bipole case made by Beveridge *et al*. (2002). This article catalogues all of the possible topological states due to four sources, and finds where bifurcations between the states take place.

The method outlined in Section 3 is readily extended to greater numbers of sources. For instance, with five balanced sources there are five possible domain graphs, as shown in Fig. 19.

It is interesting to compare the results of the balanced four-source case with those of the unbalanced three-source case obtained by Brown and Priest (1999). Their analysis centered on one source with strength 1, and two having strength ϵ. Examining the range $\epsilon < -0.5$ (so that a source added to give flux balance would have to be positive, giving two sources of either polarity), they found three types of topology: the (three source) nested, intersecting and detached states. We find analogs to all of these and, in addition, a state with a coronal null. In the Brown and Priest analysis, it seems there is no bifurcation between the nested and detached states. This is because there is no three-source analog to the global separatrix and global spine quasi-bifurcations. The assumed balancing source at infinity in the three-source case prevents the infinite growth of the separatrix domes and spine loops.

In the range $-0.5 < \epsilon < 0$, so that the balancing source would have to be negative (giving three sources of the same polarity, and one of the other), they again find three topological scenarios: the separate, enclosed and touching states. Again, we find analogs to all three.

Finally, they dealt also with three sources of the same sign (with a balancing source of the opposite sign), finding two topologies: the divided and the triangular states. These are simply disguised versions of the separate, enclosed and upright null states.

We expect that extending the analysis to force-free fields or changing the values of our fixed parameters – the positions of the three central sources and the strengths of two of them – would change the size and shape of the regions produced, but is highly unlikely to produce any fundamentally different topologies or bifurcations.

Although understanding these topologies is an important task in its own right, it will be interesting in the future to undertake numerical MHD experiments on various bifurcations that we have identified in order to determine their dynamical consequences for the Sun's atmosphere.

4

References

Aulanier, G., Démoulin, P., Schmieder, B., Fang, C. and Tang, Y., "Magnetohydrostatic model of a bald-patch flare", *Solar Phys.* **183**, 369 (1998).

Berger T.E., Löfdahl, M.G., Shine R.A. and Title, A.M., "Measurements of solar magnetic element motion from high resolution filtergrams", *Astrophys. J.* **495**, 973 (1998).

Beveridge, C., Priest, E.R. and Brown, D.S., "Magnetic topologies due to two bipolar regions", *Solar Phys.* **209**, 333 (2002).

Brown, D.S. and Priest, E.R., "Topological bifurcations in three-dimensional magnetic fields", *Proc. Roy. Soc. Lond.* A **455**, 3931 (1999).

Brown, D.S. and Priest, E.R., "Topological bifurcations and similarities between force-free and potential models of coronal magnetic fields", *Solar Phys.* **194** 197 (2000).

Brown, D.S. and Priest, E.R., "The topological behaviour of 3D null points in the Sun's corona", *Astron. Astrophys.* **367**, 339 (2001)

Démoulin, P., Hénoux, J.-C. and Mandrini, C.H., "Development of a topological model for solar flares", *Solar Phys.* **139**, 105 (1992).

Démoulin, P., Hénoux, J.-C. and Schmieder, B., "3-D structure of flaring active regions", In: *Understanding Solar Active Phenomena*. International Academic Publishers & World Publishing Corporation, Beijing, China (1999).

Fletcher, L., Metcalf, T.R., Alexander, D., Ryder, L.A., Brown, D.S. and Nightingale, R.W., "Multi-wavelength observations of an M1.9 class flare – evidence for spine and fan reconnection", *Astrophys. J.* **554**, 451 (2001).

Galsgaard, K. and Nordlund, Å, "Boundary shearing of an initially homogeneous magnetic field", *J. Geophys. Res.* **102**, 231 (1997).

Galsgaard, K., Parnell, C.E. and Blaizot, J., "Elementary heating events – Magnetic interactions between two flux sources", *Astron. Astrophys.* **362**, 383 (2000).

Gorbachev, V.S., Kel'ner, S.R., Somov, B.V. and Shverts, A.S., "A new topological approach to the question of the trigger for solar flares", *Soviet Astron.* **32**, 308 (1988).

Inverarity, G. and Priest, E.R., "Magnetic null points due to multiple sources of solar photospheric flux", *Solar Phys.* **186**, 99 (1999).

Lau, Y.T., "Magnetic nulls and topologies in a class of solar flare models", *Solar Phys.* **148**, 301 (1993).

Lau, Y.T. and Finn, J.M., "Three-dimensional kinematic reconnection in the presence of field nulls and closed field lines", *Astrophys. J.* **350**, 672 (1990).

Longcope, D.W., "Topology and current ribbons: a model for current, reconnection and flaring in a complex, evolving corona", *Solar Phys.* **169**, 91–121 (1996).

Longcope, D.W. and Klapper, I., "A general theory of connectivity and current sheets in coronal magnetic fields anchored to discrete sources", *Astrophys. J.* **579**, 468 (2002).

Molodenskii, M.M. and Syrovatskii, S.I., "Magnetic fields of active regions and their zero points", *Soviet Astron.* **21**, 734 (1977).

Parnell, C.E., "A model of the solar magnetic carpet", *Solar Phys.* **200**, 23–45 (2001)

Parnell, C.E., Smith, J.M., Neukirch, T. and Priest, E.R., "The structure of three-dimensional magnetic neutral points", *Phys. Plasmas* **3**, 759 (1996).

Priest, E.R. and Titov, V.S., "Magnetic reconnection at three-dimensional null points", *Phil. Trans. Rog. Soc. Lond.* A **354**, 2951 (1996).

Priest, E.R., Bungey, T.N. and Titov, V.S., "The 3D topology interaction of complex magnetic flux systems", *Geophys. Astrophys. Fluid Dynam.* **84**, 127 (1997).

Titov, V.S. and Hornig, G., "Magnetic connectivity of coronal fields: geometrical versus topological description", *Adv. Space Res.* **29**, 1087 (2002).

Titov, V.S., Hornig, G. and Démoulin, P., "The theory of magnetic connectivity in the solar corona", *J. Geophys. Res.* **107**, A8 (2002).

AUTHOR QUERIES

JOURNAL ID: GGAF - 41015

QUERY NUMBER	QUERY
1	Please check if the placement of Fig. 1 as per editorial marking is OK?
2	Sentence seems to be ambiguous. Please check.
3	Please check the change made.
4	Please expand the abbreviation “MHD” on its first occurrence.